

# Proton Abstraction Reaction, Steady-State Kinetics, and Oxidation–Reduction Potential of Human Glutaryl-CoA Dehydrogenase<sup>†</sup>

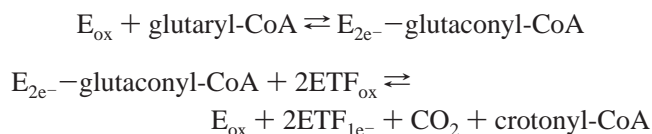
Timothy M. Dwyer,<sup>‡,§</sup> K. Sudhindra Rao,<sup>‡,§</sup> Stephen I. Goodman,<sup>‡</sup> and Frank E. Frerman<sup>\*,‡,||</sup>

Departments of Pediatrics and Pharmaceutical Sciences, University of Colorado Health Sciences Center, Denver, Colorado 80262

Received March 28, 2000; Revised Manuscript Received June 15, 2000

**ABSTRACT:** Glutaryl-CoA dehydrogenase catalyzes the oxidation of glutaryl-CoA to crotonyl-CoA and CO<sub>2</sub> in the mitochondrial degradation of lysine, hydroxylysine, and tryptophan. We have characterized the human enzyme that was expressed in *Escherichia coli*. Anaerobic reduction of the enzyme with sodium dithionite or substrate yields no detectable semiquinone; however, like other acyl-CoA dehydrogenases, the human enzyme stabilizes an anionic semiquinone upon reduction of the complex between the enzyme and 2,3-enoyl-CoA product. The flavin potential of the free enzyme determined by the xanthine–xanthine oxidase method is –0.132 V at pH 7.0, slightly more negative than that of related flavoprotein dehydrogenases. A single equivalent of substrate reduces 26% of the dehydrogenase flavin, suggesting that the redox equilibrium on the enzyme between substrate and product and oxidized and reduced flavin is not as favorable as that observed with other acyl-CoA dehydrogenases. This equilibrium is, however, similar to that observed in isovaleryl-CoA dehydrogenase. Comparison of steady-state kinetic constants of glutaryl-CoA dehydrogenase with glutaryl-CoA and the alternative substrates, pentanoyl-CoA and hexanoyl-CoA, suggests that the  $\gamma$ -carboxyl group of glutaryl-CoA stabilizes the enzyme–substrate complex by at least 5.7 kJ/mol, perhaps by interaction with Arg94 or Ser98. Glu370 is positioned to function as the catalytic base, and previous studies indicate that the conjugate acid of Glu370 also protonates the transient crotonyl-CoA anion following decarboxylation [Gomes, B., Fendrich, G., and Abeles, R. H. (1981) *Biochemistry* 20, 3154–3160]. Glu370Asp and Glu370Gln mutants of glutaryl-CoA dehydrogenase exhibit 7% and 0.04% residual activity, respectively, with human electron-transfer flavoprotein; these mutations do not grossly affect the flavin redox potentials of the mutant enzymes. The reduced catalytic activities of these mutants can be attributed to reduced extent and rate of substrate deprotonation based on experiments with the nonoxidizable substrate analogue, 3-thiaglutaryl-CoA, and kinetic experiments. Determination of these fundamental properties of the human enzyme will serve as the basis for future studies of the decarboxylation reaction which is unique among the acyl-CoA dehydrogenases.

Glutaryl-CoA dehydrogenase (GCD)<sup>1</sup> catalyzes the oxidation and decarboxylation of glutaryl-CoA to crotonyl-CoA and carbon dioxide in the oxidative pathways for lysine, hydroxylysine, and tryptophan (1–3)



where ETF is the electron-transfer flavoprotein, the physiological oxidant of the dehydrogenase (1). The decarboxylation reaction is unique among the acyl-CoA dehydroge-

nases. Mammalian GCD is a homotetramer of identical subunits ( $M_r \approx 43$  kDa) and contains 1 equiv of FAD per subunit (1). Previously, the pig liver and human liver GCDs were partially characterized by Lenich and Goodman (1); however, all information regarding the redox behavior and catalytic mechanism of this dehydrogenase has been obtained with bacterial GCDs isolated from *Pseudomonas fluorescens* and *Paracoccus denitrificans* (3–5).

A cDNA encoding the human dehydrogenase was recently cloned, and the protein was expressed in *Escherichia coli* (6). Expression of the enzyme has permitted the preliminary characterization of a number of mutations from patients with glutaric acidemia type I, an inherited neurologic disease, resulting from mutations in GCD (7, 8). In this paper, residues are numbered according to the mature protein

<sup>†</sup> This work was supported by a grant from the U.S. Public Health Service (NS 39339) and in part by a grant from the Children's Hospital Research Institute.

\* Address correspondence to this author at the Department of Pediatrics, Box C233, University of Colorado Health Sciences Center, 4200 E. 9th Ave., Denver, CO 80262. Phone: 303-315-7269. Fax: 303-315-8080. E-mail: frank.frerman@uchsc.edu.

<sup>‡</sup> Department of Pediatrics.

<sup>§</sup> These individuals contributed equally to these investigations.

<sup>||</sup> Department of Pharmaceutical Sciences.

<sup>1</sup> Abbreviations: GCD, glutaryl-CoA dehydrogenase; ETF, electron-transfer flavoprotein; AMPD-HCl, 2-amino-2-methyl-1,3-propanediol hydrochloride; MES, 2-(N-morpholino)ethanesulfonic acid; Hepes, N-(2-hydroxyethyl)piperazine-N'-2-ethanesulfonic acid; bis-Tris-HCl, bis(2-hydroxyethyl)iminotris(hydroxymethyl)methane hydrochloride; Tris-HCl, tris(hydroxymethyl)aminomethane hydrochloride; PMS, phenazine methosulfate; DCPIP, 2,6-dichlorophenolindophenol; FcPF<sub>6</sub>, ferrocenium hexafluorophosphate; EDTA, ethylenediaminetetraacetic acid.

sequence for reference to the three-dimensional structure (9); the 44 amino acid mitochondrial targeting sequence is not included in the numbering (6). The sequence similarity between human GCD and most other acyl-CoA dehydrogenases suggests that Glu370 in the mature sequence is the base that abstracts the *pro-R*  $\alpha$ -hydrogen as a proton from the acyl-CoA substrate (2). Also, X-ray crystallographic studies indicate that this residue is correctly positioned to act as the catalytic base (9). On the basis of the mechanistic studies of Abeles and co-workers, the conjugate acid of Glu370 also protonates the  $\gamma$ -carbon of the crotonyl-CoA anion following decarboxylation of glutacetyl-CoA, the presumed enzyme-bound intermediate, to yield crotonyl-CoA (2).

In this study, we investigated the steady-state turnover of purified, recombinant, human GCD with glutaryl-CoA and alternate substrates and determined the redox potentials of the wild-type, Glu370Asp, and Glu370Gln dehydrogenases. The binding of several nonoxidizable substrate analogues was studied to obtain additional information regarding proton abstraction by the dehydrogenase. The effects of mutations of the glutamate catalytic base of several acyl-CoA dehydrogenases have been determined (10–13). However, because of the dual role of the catalytic base suggested by the work of Abeles and co-workers (2), we studied the properties of two site-directed mutants of the enzyme, Glu370Asp and Glu370Gln. These studies were conducted prior to further investigations of the decarboxylation of the  $\gamma$ -carboxylate of glutaryl-CoA and protonation of the  $\gamma$ -carbon of the intermediate crotonyl-CoA anion.

## EXPERIMENTAL PROCEDURES

**Materials.** Indigo disulfonate, ferrocenium hexafluorophosphate (FcPF<sub>6</sub>), and valeric anhydride were purchased from Aldrich. Thiodiglycolic anhydride was purchased from Lancaster. CoASH, hexanoyl-CoA, crotonyl-CoA, glutaric anhydride, and acetoacetyl-CoA were obtained from Sigma. Other reagents were purchased from commercial sources and were the best grade available.

Human ETF was purified as previously described (14). Milk xanthine oxidase was the gift of Dr. Russ Hille, Ohio State University.

**Synthetic Procedures.** Glutaryl-CoA, pentanoyl-CoA (valeryl-CoA), and 3-thiaglutaryl-CoA were synthesized by reaction of their anhydrides with CoASH (15). All synthetic acyl-CoA esters were purified by high-performance liquid chromatography on a semipreparative reversed-phase C-18 (10  $\times$  250 mm) column with 50 mM potassium phosphate buffer, pH 5.3, and methanol (95:5 v/v) and desalted on a column (1  $\times$  100 cm) of Sephadex G-10 eluted with water. CoA esters were quantitated using  $\epsilon_{260\text{nm}} = 16.4 \times 10^3 \text{ M}^{-1} \text{ cm}^{-1}$  (16).

**Purification of Glutaryl-CoA Dehydrogenase.** Human wild-type GCD was purified as previously described (6), except that an additional chromatography step was included. In this final step, the protein was chromatographed on a Source 15Q (Pharmacia) column (1  $\times$  8 cm) equilibrated in 50 mM potassium phosphate, pH 7.0, and 5% glycerol. The enzyme was eluted with a 50 mL linear gradient to 250 mM potassium phosphate, pH 7.0, and 5% glycerol. This procedure yielded a protein with an  $A_{269\text{nm}}/A_{447\text{nm}}$  ratio of 5.0–5.1. The mutant dehydrogenases were purified by the same

procedure. The  $A_{269\text{nm}}/A_{446\text{nm}}$  ratio of the Glu370Asp mutant was 5.2, and the  $A_{268\text{nm}}/A_{448\text{nm}}$  ratio of the Glu370Gln mutant dehydrogenase was 5.9. The purity of all preparations was assessed by absorption spectra and SDS–PAGE. Although the  $A_{268\text{nm}}/A_{448\text{nm}}$  ratio was higher for the Glu370Gln mutant protein than the corresponding ratio for the other proteins, it was homogeneous as judged by SDS–PAGE so that the slightly higher  $A_{268\text{nm}}/A_{448\text{nm}}$  ratio may indicate some loss of FAD.

**Enzyme Assays.** Assays performed to determine the relative activities of native and mutant glutaryl-CoA dehydrogenases were conducted in 10 mM potassium phosphate, pH 7.0. The dehydrogenase was assayed with phenazine methosulfate (PMS), 2 mM, and 2,6-dichlorophenolindophenol (DCPIP), 0.05 mM, as the terminal electron acceptor ( $\epsilon_{600\text{nm}} = 2.1 \times 10^4 \text{ M}^{-1} \text{ cm}^{-1}$ ) (17) or fluorometrically with human ETF, 5  $\mu\text{M}$  (18). The enzyme was also assayed with FcPF<sub>6</sub>, 200  $\mu\text{M}$ , as the electron acceptor using  $\epsilon_{300\text{nm}} = 4.3 \times 10^3 \text{ M}^{-1} \text{ cm}^{-1}$  (19). Steady-state kinetic constants of wild-type dehydrogenases with glutaryl-CoA, hexanoyl-CoA, and pentanoyl-CoA as substrates were conducted in the same buffer as above with the acyl-CoA esters as varied substrates and 200  $\mu\text{M}$  FcPF<sub>6</sub> as the electron acceptor. The steady-state kinetic constants of Glu370Asp GCD with glutaryl-CoA were determined with the same assay.

**Redox Methods.** Glutaryl-CoA dehydrogenase was reduced under anaerobic conditions with sodium dithionite or by irradiation in the presence of 10 mM EDTA and 0.5  $\mu\text{M}$  5-deaza-3-propylriboflavin (20). Dithionite was standardized immediately before use by titration of cytochrome *c*.

The redox potentials of wild-type GCD and the Glu370Asp and Glu370Gln mutants were determined by the xanthine–xanthine oxidase method (21). Reaction mixtures contained 50 mM potassium phosphate at pH 7.6, 7.0, or 6.4, 10% glycerol, 250  $\mu\text{M}$  xanthine, 2  $\mu\text{M}$  benzyl viologen, 10  $\mu\text{M}$  dehydrogenase, 90 nM xanthine oxidase, and 10  $\mu\text{M}$  indigo disulfonate. Reduction of indigo disulfonate was followed at 616 nm, and the reduction of the enzymes was followed at 454 nm, an isosbestic point for the dye.

Literature values for the potentials of indigo disulfonate at pH 7.6 [–0.121 V (22)], and 6.4 [–0.059 V (4)] were assumed. The potential of the dye at pH 7.0, –0.108 V, was determined by cyclic voltammetry in 50 mM potassium phosphate, pH 7.0, using a gold electrode and an Omni 90 potentiostat with a scan rate of 0.1 V/s at room temperature.

**Titration with Substrate and Substrate Analogues.** In titrations of GCDs with substrate, the enzymes, in 10 mM potassium phosphate, pH 7.2, and 10% glycerol, were made anaerobic by 20 cycles of alternate evacuation and purging with argon; 2 units of glucose oxidase and 36 units of catalase were added to remove residual oxygen. The enzymes were then titrated with an anaerobic solution of glutaryl-CoA.

Spectrophotometric titrations of wild-type GCD and mutant GCDs with 3-thiaglutaryl-CoA and acetoacetyl-CoA were performed at the indicated pH values at 23 °C. Difference molar extinction coefficients at suitable wavelengths (see text for details) were determined by curve fitting absorbance changes as a function of total ligand concentration to a hyperbolic equation. Using this extinction coefficient, the binding data were calculated and analyzed by curve fitting to the equation (23)

$$\nu = \frac{n[L]_{\text{free}}}{K_d + [L]_{\text{free}}} \quad (1)$$

where  $\nu$  is the moles of ligand bound per mole of flavin,  $n$  is the maximum number of binding sites, and  $K_d$  is the dissociation constant. The pH dependence of  $\epsilon_{825\text{nm}}$  for the interaction of GCD with 3-thiaglutaryl-CoA was further analyzed to yield  $pK_a$  values by curve fitting to the equation (24)

$$\epsilon_H = \frac{\epsilon_{\text{HA}}[H^+] + \epsilon_A K_a}{K_a + [H^+]} \quad (2)$$

where  $\epsilon$  is the molar extinction coefficient,  $K_a$  is the association constant ( $pK_a = -\log K_a$ ), and  $[H^+]$  is the proton concentration ( $\text{pH} = -\log [H^+]$ ). The subscripts H, HA, and  $A^-$  refer to the observed value at a particular pH, the value for the un-ionized state, and the value for the singly ionized state, respectively. All titration data were analyzed using KaleidaGraph version 3.08 software. The binding of acetoacetyl-CoA to the wild-type dehydrogenase at pH 6.4 was analyzed similarly from spectral data at 322 nm.

**Site-Directed Mutagenesis.** The mutations, Glu370Gln and Glu370Asp GCDs, were generated using the Quickchange mutagenesis system (Stratagene) according to the manufacturer's instructions. The mutagenized plasmid was sequenced in the region of the mutation to verify introduction of the mutation. Cassettes containing the mutated site were removed by digestion with *Pst*I and *Hind*III and ligated into the wild-type plasmid that had been digested with the same endonucleases. The mutant cassette and digested wild-type plasmid were purified by electrophoresis prior to ligation. The resulting expression vectors were then sequenced across junctions and through the mutated cassette to demonstrate the mutations and absence of unwanted mutations. No unwanted mutations were detected. DNA was sequenced by the dideoxynucleotide method (25) using the Alf Express System (Pharmacia).

## RESULTS

**Absorption Spectra.** Figure 1 shows the absorption spectra of the three oxidation states of wild-type human GCD. The maxima of the oxidized enzyme are 269, 369, and 447 nm (5.0:0.6:1.0). The extinction coefficient of the bound, oxidized flavin at 447 nm is  $14.5 \times 10^3 \text{ M}^{-1} \text{ cm}^{-1}$ , determined by release of the flavin from the protein with 0.1% sodium dodecyl sulfate (26). The near-UV transition (369 nm) of the wild-type dehydrogenase shows some resolution with a small shoulder to lower wavelengths. The unliganded protein does not stabilize a significant amount of semiquinone (see below); however, the dehydrogenase–crotonyl-CoA complex does stabilize an anionic semiquinone ( $\epsilon_{388\text{nm}} = 19.8 \times 10^3 \text{ M}^{-1} \text{ cm}^{-1}$  and  $\epsilon_{447\text{nm}} = 6.5 \times 10^3 \text{ M}^{-1} \text{ cm}^{-1}$ ) (see below). Although it is difficult to determine with absolute certainty (27), the absorption spectrum of the two-electron reduced state suggests that human GCD stabilizes a neutral dihydroquinone ( $\epsilon_{447\text{nm}} = 1.9 \times 10^3 \text{ M}^{-1} \text{ cm}^{-1}$ ).

The spectrum of oxidized Glu370Asp GCD is almost identical to that of the wild type except that the maximum in the visible region is slightly shifted to 446 nm ( $\epsilon_{446\text{nm}} = 14.3 \times 10^3 \text{ M}^{-1} \text{ cm}^{-1}$ ). The absorption maxima are 269, 369,

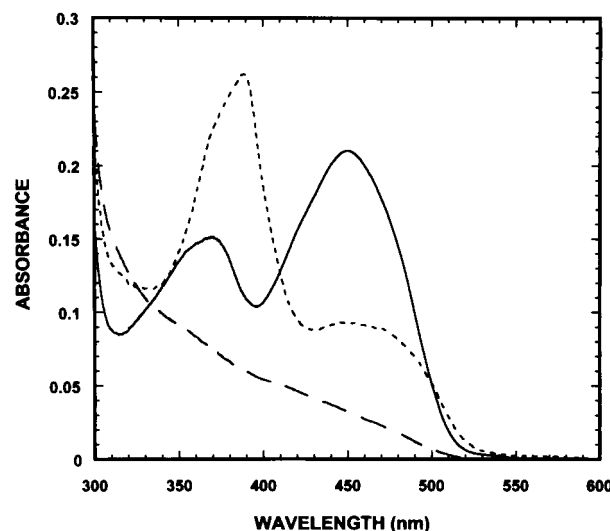


FIGURE 1: Visible absorption spectra of the oxidation states of wild-type glutaryl-CoA dehydrogenase flavin. Spectra were determined with  $14.5 \mu\text{M}$  GCD in the oxidized (—), semiquinone (---), and dihydroquinone (— · —) forms. The semiquinone was produced by anaerobic reduction of GCD in the presence of a 10% molar excess of crotonyl-CoA; the complex was irradiated in the presence of 10 mM EDTA and  $0.5 \mu\text{M}$  5-deaza-3-propylriboflavin. Maximum dihydroquinone was produced by complete anaerobic reduction of the uncomplexed wild-type GCD by irradiation in the presence of EDTA and the deazaflavin as above.

and 446 nm (5.2:0.58:1.0). The absorption spectrum of the Glu370Gln mutant exhibited absorption maxima at 268, 369, and 448 nm (5.9:0.73:1.0) with  $\epsilon_{448\text{nm}} = 13.2 \times 10^3 \text{ M}^{-1} \text{ cm}^{-1}$ .

**Redox Behavior and Oxidation–Reduction Potentials of the Dehydrogenases.** Reduction of the dehydrogenase flavin with sodium dithionite proceeds without formation of detectable amounts of a flavin semiquinone. The isosbestic point at 339 nm (Figure 2) is maintained throughout the titration, further indicating that only the oxidized and dihydroquinone oxidation states are present during the titration. Reductions of Glu370Asp and Glu370Gln mutant GCDs proceed identically (data not shown). Like *P. denitrificans* GCD and medium chain acyl-CoA dehydrogenase (4, 28), wild-type GCD stabilizes an anionic semiquinone when the enoyl-CoA product, crotonyl-CoA, is bound (Figure 1). Figure 3 shows the reduction of the wild-type dehydrogenase flavin in an anaerobic titration with glutaryl-CoA. The isosbestic point at 335 nm is maintained throughout the titration, and the absorbance at 560 nm increases in parallel with flavin reduction due to formation of a charge-transfer species between the enoyl-CoA intermediate, glutaconyl-CoA, and the reduced flavin. Addition of substrate, equimolar with flavin, results in the reduction of 23–26% of the dehydrogenase flavin at pH 7.0. Addition of a 10-fold excess of substrate reduces 63% of the flavin at pH 7.0. The Glu370Asp mutant behaved similarly.

The oxidation–reduction potentials of the wild-type GCD flavin were determined at pH 7.6 and 7.0 for comparison with medium-chain acyl-CoA dehydrogenase (22, 29) and at pH 6.4 for comparison with previous experiments with *P. denitrificans* GCD (4). A published value for the oxidation–reduction potential,  $-0.125 \text{ V}$ , of indigo disulfonate at pH 7.0 (30) appeared inconsistent with literature values of the potentials of the dye at pH 6.4 [ $-0.059 \text{ V}$  (4)] and



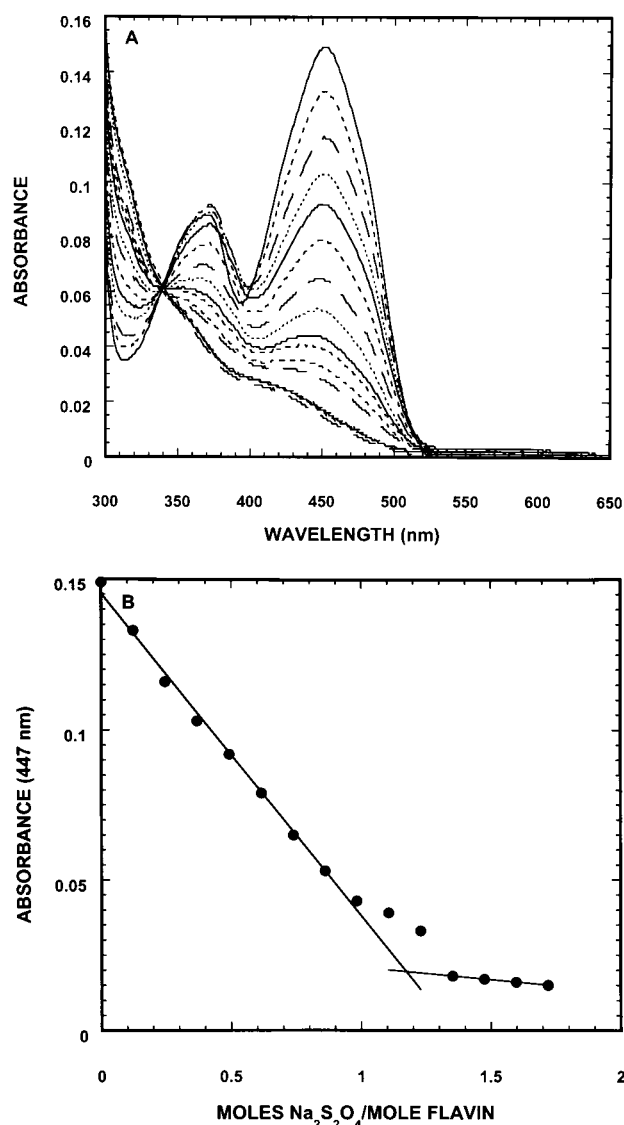


FIGURE 2: Reduction of wild-type human glutaryl-CoA dehydrogenase with sodium dithionite. (A) Spectra of wild-type GCD during the titration with sodium dithionite. (B) Data from the titration of wild-type GCD in panel A showing the dependence of absorption at 447 nm as a function of dithionite added; the dithionite was standardized by titration of cytochrome *c*.

pH 7.6 [ $-0.121$  V (22)]. Therefore, we determined the potential of indigo disulfonate in 50 mM potassium phosphate, pH 7.0, by cyclic voltammetry. The experimentally determined potential,  $-0.108$  V at pH 7.0, was used to calculate the dehydrogenase flavin potentials at pH 7.0. The potentials of the wild-type dehydrogenase flavin are given in Table 1. The values shown in Table 1 are similar to, but slightly more negative than, those determined for other acyl-CoA dehydrogenases (29, 31), including human long-chain acyl-CoA dehydrogenase,  $-0.124$  V (32), determined at pH 7.6, and the potential of *P. denitrificans* GCD,  $-0.059$  V, determined at pH 6.4 (4). The data in Table 1 for wild-type GCD show a slope of  $-0.054$  V/pH. Although this is a relatively narrow pH range, the slope indicates a  $2e^-/2H^+$  transfer as was the case with pig liver medium-chain acyl-CoA dehydrogenase (29).

The potentials of the Glu370Asp and Glu370Gln mutant dehydrogenase flavins were also determined at pH 7.0 with

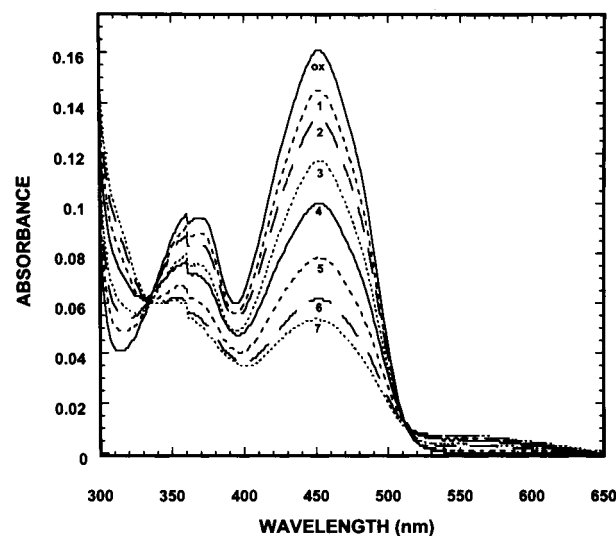


FIGURE 3: Anaerobic titration of glutaryl-CoA dehydrogenase with glutaryl-CoA. The oxidized dehydrogenase, 8.9 nmol (ox), was titrated with glutaryl-CoA, (1) 4.3 nmol, (2) 8.6 nmol, (3) 17.2 nmol, (4) 34 nmol, (5) 70 nmol, (6) 130 nmol, and (7) 310 nmol.

Table 1: Oxidation–Reduction Potentials of Wild-Type and Mutant Glutaryl-CoA Dehydrogenases

enzyme	$E_m$ (V)		
	pH 6.4	pH 7.0	pH 7.6
wild-type GCD	$-0.090 \pm 0.003^a$	$-0.132 \pm 0.008$	$-0.156 \pm 0.003$
Glu370Asp GCD	ND <sup>b</sup>	$-0.131 \pm 0.005$	ND <sup>b</sup>
Glu370Gln GCD	ND <sup>b</sup>	$-0.127 \pm 0.001$	ND <sup>b</sup>

<sup>a</sup> Mean and standard error of two to four determinations. <sup>b</sup> These potentials were not determined.

Table 2: Activities of Wild-Type, Glu370Asp, and Glu370Gln Glutaryl-CoA Dehydrogenases with Artificial and Physiological Electron Acceptors

electron acceptor	activity ( $s^{-1}$ )		
	wild type	Glu370Asp (mutant/wild type)	Glu370Gln (mutant/wild type)
PMS–DCPIP	4.8 <sup>a</sup>	0.16 (0.033)	0.0038 (0.0008)
FcPF <sub>6</sub>	7.5	0.32 (0.042)	$\leq 0.03$ ( $\leq 0.004$ )
ETF	5.7	0.39 (0.068)	0.0026 (0.0004)

<sup>a</sup> Activities are expressed as turnover under the standard conditions described in Experimental Procedures.

indigo disulfonate as the indicator. The potentials of  $-0.131$  and  $-0.128$  V at pH 7.0 for the Glu370Asp and Glu370Gln mutants, respectively, were essentially the same as those of the wild-type protein, indicating that the mutations affect the flavin potential very little (Table 1).

**Steady-State Kinetics.** Table 2 shows the activity of wild-type GCD and the Glu370Asp and Glu370Gln mutants at pH 7.0 assayed with different electron acceptors. Activities were determined at 30  $\mu$ M glutaryl-CoA substrate and are consistent with the assignment of Glu370 as the catalytic base in GCD. The residual activity of the Glu370Asp mutant is comparable to that previously reported for the similar Glu376Asp mutant of medium-chain acyl-CoA dehydrogenase (33). When assayed by the sensitive fluorometric assay with ETF as the electron acceptor, the residual activity of the Glu370Gln mutant is 0.04%, similar to that of the corresponding mutant (Glu261Gln) of long-chain acyl-CoA

Table 3: Steady-State Kinetic Constants of Wild-Type Glutaryl-CoA Dehydrogenase<sup>a</sup>

substrate	$K_m$ ( $\mu$ M)	$k_{cat}$ ( $s^{-1}$ )	$k_{cat}/K_m$ ( $s^{-1} \mu M^{-1}$ )
glutaryl-CoA	$2.5 \pm 0.7$	$8.1 \pm 1.1$	3.2
hexanoyl-CoA	$25.6 \pm 3.9$	$12.6 \pm 2.1$	0.49
pentanoyl-CoA	$49.9 \pm 4.2$	$12.0 \pm 1.2$	0.24

<sup>a</sup> Assayed with 200  $\mu$ M ferrocenium hexafluorophosphate as electron acceptor at pH 7.0, 25 °C.

dehydrogenase (12). Also, the rate of flavin bleaching by substrate of the Glu376Gln mutant of medium-chain acyl-CoA dehydrogenase was 0.02% of that of pig kidney medium-chain acyl CoA dehydrogenase (34). Thus, the activities of the two GCD mutants are comparable to those reported for similar mutations in other acyl-CoA dehydrogenases and are consistent with the hypothesis that Glu370 is the catalytic base in human GCD (9).

The steady-state kinetic constants of wild-type GCD with glutaryl-CoA as substrate and with the alternative substrates, hexanoyl-CoA and pentanoyl-CoA, at pH 7.0 are shown in Table 3. The values of  $k_{cat}$  and  $K_m$  for glutaryl-CoA of wild-type GCD are similar to those reported for the pig liver enzyme with pig liver ETF as the electron acceptor (1). The data in Table 3 also show that oxidation and decarboxylation are not obligatorily coupled because the *n*-alkyl acyl-CoA esters are reasonably good substrates. The  $K_m$  values for pentanoyl-CoA and hexanoyl-CoA also suggest that the  $\gamma$ -carboxylate of glutaryl-CoA contributes significantly to substrate binding. As shown in Table 2, the Glu370Asp dehydrogenase has only 3–7% of the wild-type activity when assayed with all three of the conventional enzyme assays at pH 7.0 and with 30  $\mu$ M glutaryl-CoA as the substrate. At pH 7.0 with FcPF<sub>6</sub> as the electron acceptor, the  $K_m$  of the Glu370Asp dehydrogenase for glutaryl-CoA is 2.0  $\mu$ M, which is essentially identical to the wild-type dehydrogenase;  $k_{cat}$  is 0.56  $s^{-1}$ , about 7% of the wild-type value.

The activities and difference between the activities of wild-type GCD and the Glu370Asp mutant are pH dependent. The pH dependence of activity of the two enzymes is shown in Figure 4 and is expressed as a turnover number because assays were conducted with 200  $\mu$ M glutaryl-CoA. The  $K_m$  of the wild-type dehydrogenase for glutaryl-CoA is almost constant between pH 6 and pH 8. However, the  $K_m$  of the wild type increases to 36  $\mu$ M at pH 9, so that the concentration of substrate is still about 6-fold greater than  $K_m$  in this pH region. As shown in Figure 4A, wild-type GCD exhibits maximal activity (17  $s^{-1}$ ) at pH 8.8. The data were best fit by assuming two ionizable groups with  $pK_a$ s of 6.3 and 7.9. In contrast, the Glu370Asp dehydrogenase has maximal activity (2.5  $s^{-1}$ ) at pH 8.5 with a single ionizable group ( $pK_a = 7.6$ ) (Figure 4B). The decrease in activity at pH 9 is not due to instability of the enzyme or FcPF<sub>6</sub> under steady-state conditions; however, the enzyme is unstable when held below pH 6 and above pH 9 for more than 15 min.

**Binding of Substrate Analogues and Proton Abstraction.** Abstraction of the  $\alpha$ -proton of acyl-CoAs by the GCDs was analyzed by titration of the enzymes with the nonoxidizable substrate analogues, acetoacetyl-CoA and 3-thiaglutaryl-CoA. Figure 5 shows a titration of the wild-type enzyme with acetoacetyl-CoA. Prominent spectral features in the titration

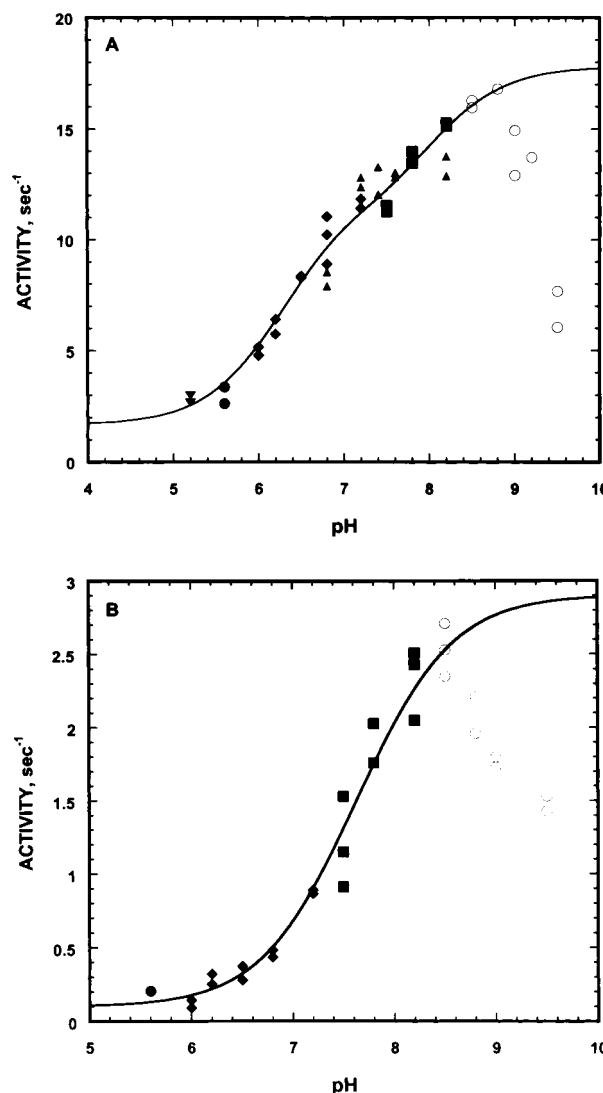


FIGURE 4: Dependence of the activities of wild-type and Glu370Asp GCD on pH. The activities expressed as turnover numbers of wild-type (A) and Glu370Asp GCD (B) were determined over a pH range of 5.2–9.5 in the presence of 200  $\mu$ M glutaryl-CoA with FcPF<sub>6</sub> as the terminal electron acceptor. Reaction mixtures contained the following buffers, each at a final concentration of 10 mM containing 100 mM NaCl: pH 5.2, sodium citrate ( $\blacktriangledown$ ); pH 5.6, MES K<sup>+</sup> ( $\bullet$ ); pH 6–7.2, bis-Tris-HCl ( $\blacklozenge$ ); pH 7.6–8.2, Hepes ( $\blacksquare$ ); pH 7.5–8.2, Tris-HCl ( $\blacktriangle$ ); and pH 8.5–9.5, AMPD-HCl ( $\circ$ ). For the wild-type dehydrogenase, the data were best fit to eq 2 between the limits of 1.7 and 12.6  $s^{-1}$  to calculate a  $pK_a$  of 6.3 and between 10 and 17.8  $s^{-1}$  to calculate a  $pK_a$  of 7.9. For the Glu370Asp mutant protein the  $pK_a$  of 7.6 was calculated using the limits of 0.1 and 2.9  $s^{-1}$ .

are increased absorption at 322 nm and in the 550 nm region and decreased absorbance at the maximum, 447 nm, with a slight red shift to 451 nm. The 322 nm absorbance is likely due to formation of the enolate of acetoacetyl-CoA on the enzyme since the pH of the buffer is at least 3 pH units below the  $pK_a$  of the  $\alpha$ -proton of acetoacetyl-CoA in solution (35). The absorption at 550 nm is attributed to formation of a charge-transfer complex between the negatively charged enolate and the electron-deficient oxidized flavin (36). The apparent  $K_d$  of this binary complex is 0.48  $\mu$ M, calculated from the increase of absorbance at 322 nm, with 1 equiv of the 3-oxoacyl-CoA bound per flavin site. Essentially identical results were obtained when  $K_d$  was calculated from the change in absorbance at 440 nm. The Glu370Asp dehydro-

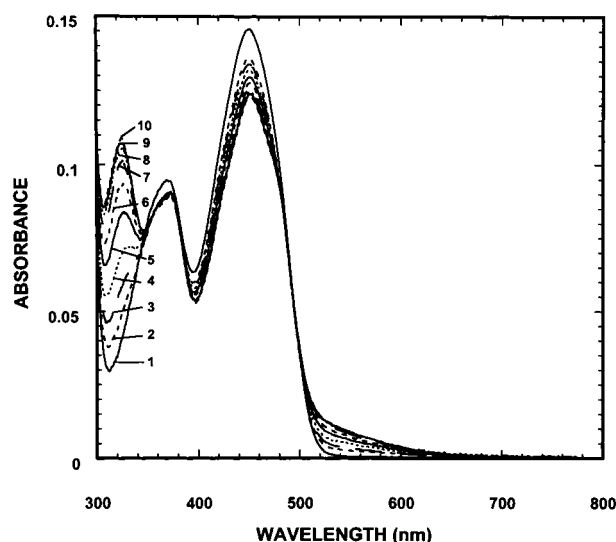


FIGURE 5: Spectrophotometric titration of wild-type glutaryl-CoA dehydrogenase with acetoacetyl-CoA. Wild-type GCD ( $8.8 \mu\text{M}$ ) was titrated with acetoacetyl-CoA in 50 mM potassium phosphate, pH 6.4, at  $25^\circ\text{C}$ . The acetoacetyl-CoA concentrations were (1) 0, (2)  $1 \mu\text{M}$ , (3)  $2 \mu\text{M}$ , (4)  $3 \mu\text{M}$ , (5)  $5 \mu\text{M}$ , (6)  $7 \mu\text{M}$ , (7)  $10 \mu\text{M}$ , (8)  $13 \mu\text{M}$ , (9)  $15.5 \mu\text{M}$ , and (10)  $18 \mu\text{M}$ .

genase does not exhibit a discrete absorption maximum in the 320 nm region when titrated with acetoacetyl-CoA; however, a  $K_d = 0.69 \mu\text{M}$  was calculated from the difference in absorbance at 440 nm due to the perturbation of the flavin upon ligand binding. Subtraction of the spectrum of the free enzyme from the spectrum of the enzyme in the presence of a 32-fold molar excess of acetoacetyl-CoA showed a peak at 310 nm, presumably due to the enolate (36). This suggests that the environment of the enolate is different in the Glu370Asp dehydrogenase and wild-type GCD. We refer to  $K_d$ s calculated from the charge-transfer bands as apparent  $K_d$ s because Tamaoki et al. (37) have shown that analogues capable of forming enolates exist as the anion (charge-transfer-inducing form) and a neutral species (charge-transfer-noninducing form) on the surface of medium-chain acyl-CoA dehydrogenase. These two forms are in equilibrium on the enzyme, and the charge-transfer absorbance does not result directly from ligand binding.

We also investigated  $\alpha$ -proton abstraction by titration of the GCDs with 3-thiaglutaryl-CoA (Figure 6). The figure shows a broad band at 800–850 nm and isosbestic points at 432 and 500 nm. At pH 7.0, an apparent  $K_d$  of  $19.3 \pm 0.8 \mu\text{M}$  was determined for the complex of 3-thiaglutaryl-CoA with human wild-type GCD. The  $K_d$  was determined from the increased absorbance at 825 nm, which, by analogy with the medium-chain acyl-CoA dehydrogenase–3-thiooctanoyl-CoA complex (38, 39), reflects formation of a charge-transfer complex between the  $\alpha$ -carbanion anion of the deprotonated analogue with the oxidized flavin. Within experimental error, the number of binding sites,  $n$ , was unity with respect to the flavin content at all pH values and with the Glu370Asp mutant determined at pH 8.0. The  $K_d$  of the wild-type protein was also calculated from the change in absorbance at 391 nm at pH 7.0. The value,  $15.3 \pm 0.9 \mu\text{M}$ , may not be significantly different from the value calculated from the charge-transfer band at 825 nm. The apparent  $K_d$  determined from  $\epsilon_{825\text{nm}}$  increases with increase in pH (Table 4). A plot of  $\epsilon_{825\text{nm}}$  as a function of pH is shown in Figure 7. From the

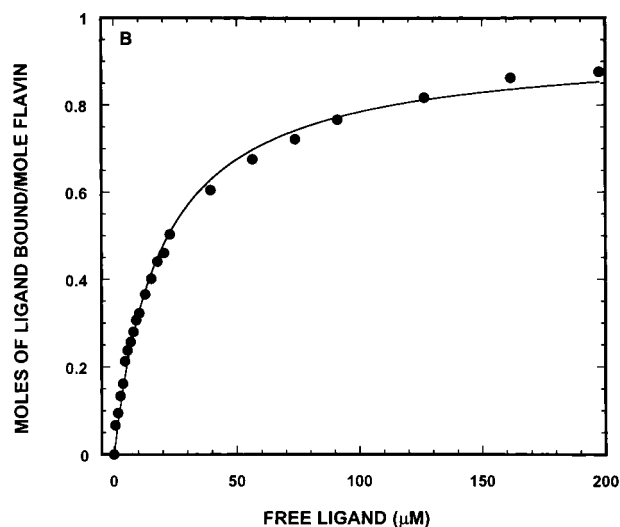
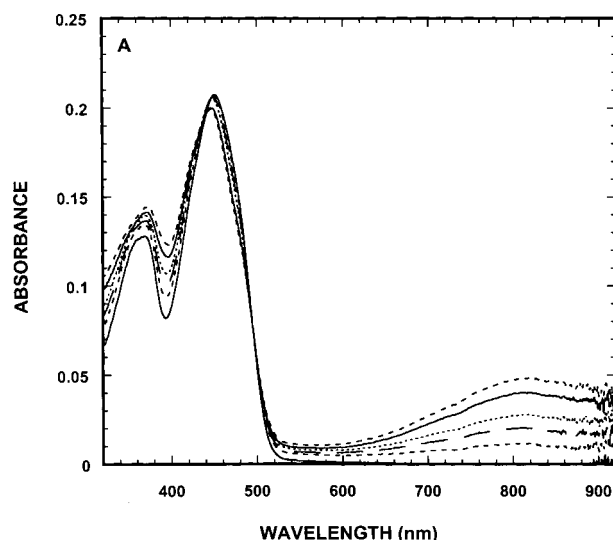


FIGURE 6: Spectrophotometric titration of wild-type GCD with 3-thiaglutaryl-CoA. (A) Absorption spectra of  $14.3 \mu\text{M}$  wild-type GCD titrated with 3-thiaglutaryl-CoA in 50 mM potassium phosphate, pH 7.0. (B) Data from the experiment in panel A plotted according to eq 1 in Experimental Procedures to determine the stoichiometry of ligand binding (0.94) and  $K_d$  ( $19.3 \mu\text{M}$ ).

Table 4: Effect of pH on the Binding of 3-Thiaglutaryl-CoA to Wild-Type Glutaryl-CoA Dehydrogenase at  $23^\circ\text{C}$

pH	$K_d$ ( $\mu\text{M}$ )	pH	$K_d$ ( $\mu\text{M}$ )
6.0	$5.7 \pm 0.6$	8.0	$32.5 \pm 2.4$
6.5	$10.7 \pm 0.5$	8.5	$45.4 \pm 4.6$
7.0 <sup>a</sup>	$19.3 \pm 0.8$	9.0	$69.0 \pm 10.0$
7.2	$22.4 \pm 0.6$	9.5	$97.6 \pm 28.3$
7.5	$28.8 \pm 0.9$		

<sup>a</sup>  $K_d = 15.3 \pm 0.9 \mu\text{M}$  for data analyzed at 391 nm at pH 7.0.

plot it is evident that at least two ionizable groups influence  $\epsilon_{825\text{nm}}$ . These two  $pK_a$  values were estimated as  $7.03 \pm 0.04$  and  $8.22 \pm 0.02$ . The data point at pH 9.5 was not included in evaluating these  $pK_a$  values due to instability of the enzyme and ligand.

Additional evidence suggesting that Glu370 acts as the base catalyst in human GCD was obtained by investigating the effect of addition of a 10-fold molar excess of 3-thiaglutaryl-CoA to the Glu370Asp mutant enzyme, assuming

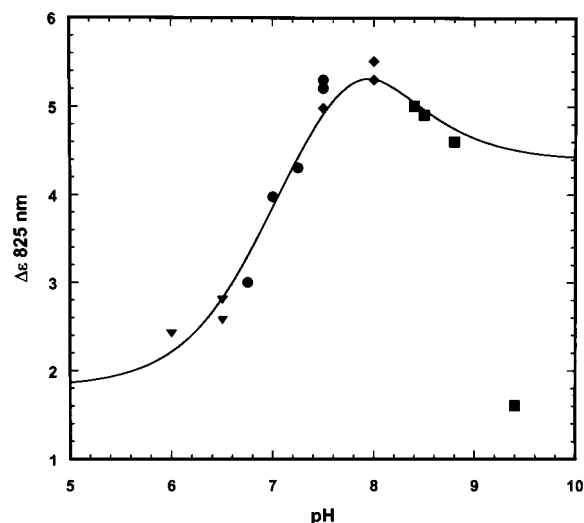


FIGURE 7: Dependence of  $\epsilon_{825\text{nm}}$  on pH. Wild-type GCD was titrated with 3-thiaglutaryl-CoA at the pH values indicated, and the maximal change in absorbance at 825 nm was plotted as a function of pH. The buffers, all 50 mM, used in the titrations were MES, pH 6.0 and 6.5 ( $\nabla$ ), potassium phosphate, pH 6.8–7.5 ( $\bullet$ ), Hepes, pH 7.5 and 8.0 ( $\blacklozenge$ ), and AMPD-HCl, pH 8.5–9.5 ( $\blacksquare$ ).

saturation (Figure 8A). The charge-transfer band at 825 nm is formed (Figure 8B), but with very low intensity ( $\epsilon_{825\text{nm}} \approx 121 \text{ M}^{-1} \text{ cm}^{-1}$  at pH 8.0), which is  $2.4 \pm 0.5\%$  of the wild-type value at pH 8.0. The  $K_d$  at pH 7.0 was determined to be  $60.5 \pm 8.4 \mu\text{M}$  by analyzing the titration data at 391 nm, where maximum absorbance changes were observed. Thus, the mutant binds the analogue with 3–4-fold lower affinity than the wild-type enzyme at pH 7.

The steady-state kinetic data and the binding of nonoxidizable substrate analogues by Glu370Asp supported the hypothesis that Glu370 functions as the catalytic base in human GCD (6, 9). However, Figure 9 shows that 3-thiaglutaryl-CoA binds to the Glu370Gln mutant GCD at pH 7 with formation of a charge-transfer species as indicated by the increased absorbance at 820 nm. From the data in Figure 9, we calculated an apparent dissociation constant of  $1.8 \pm 0.3 \mu\text{M}$ , a single binding site per FAD, and  $\epsilon_{820\text{nm}} = 1311 \pm 24 \text{ M}^{-1} \text{ cm}^{-1}$ . These results indicate that Glu370Gln GCD is still able to deprotonate the 3-thia analogue. However, the equilibrium constant for formation of the charge-transfer-inducing species, the  $\alpha$ -carbanion, is not as favorable as with the wild-type GCD, as judged by the magnitude of  $\epsilon_{825\text{nm}}$ . Consistent with these results, a charge-transfer species was also observed at pH 6.4 when a 30-fold molar excess of acetoacetyl-CoA was added to the mutant enzyme. However, in contrast to the wild-type enzyme, no change in absorbance was observed at 322 nm; rather, subtraction of the spectrum of the free enzyme from the spectrum of the enzyme–acetoacetyl-CoA complex shows a maximum at 304 nm, consistent with formation of the enolate of the 3-oxoacyl-CoA (not shown). A charge-transfer band was also detected when acetoacetyl-CoA was bound to the Glu261Gln mutant of long-chain acyl-CoA dehydrogenase at pH 7.6 (12), about 2 pH units below the  $pK_a$  of the 3-oxoacyl-CoA. Glu261 is the catalytic base in long-chain acyl-CoA dehydrogenase.

When the Glu370Gln mutant enzyme was mixed with a 10-fold molar excess of glutaryl-CoA under anaerobic conditions at 25 °C and the spectra were determined at 5 s

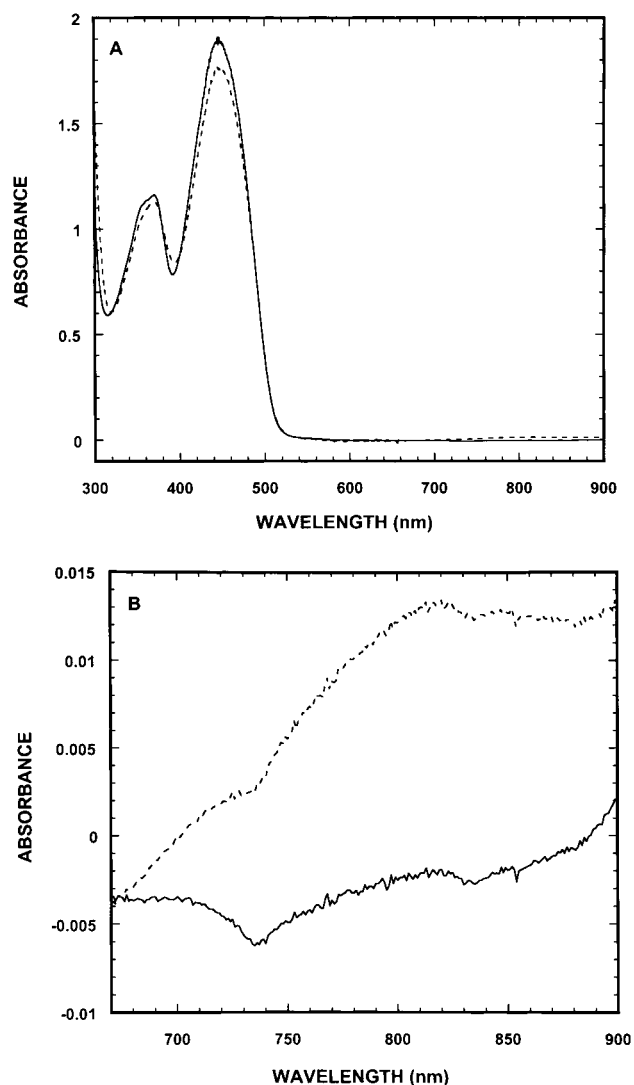


FIGURE 8: Binding of 3-thiaglutaryl-CoA by Glu370Asp GCD. The spectrum of  $136.3 \mu\text{M}$  Glu370Asp GCD (—) and Glu370Asp GCD in the presence of a 10-fold molar excess of 3-thiaglutaryl-CoA (---) was determined in 50 mM Hepes buffer, pH 8.0. The complete spectra are shown in (A), and spectra showing only the spectral region of the charge-transfer band are shown in (B).

intervals (Figure 10A), there was a decrease in absorbance at 448 nm. However, in contrast to wild-type GCD, there was no isosbestic point at 515 nm, and the spectra were continually blue shifted to a maximum of 5 nm, characteristic of substrate binding in medium-chain acyl-CoA dehydrogenase (34). Also, there was no long-wavelength absorbance characteristic of a charge-transfer species observed in the 550 nm region as found with wild-type GCD and other acyl-CoA dehydrogenases (40). In this experiment (Figure 10B), the decrease of flavin absorbance was very slow compared with the rapid reduction of the wild-type enzyme. The rate constant for the decrease in absorbance for the Glu370Gln mutant was  $0.02 \text{ s}^{-1}$ , and the decrease in absorbance at 448 nm was constant after 40 min. Finally, glutaryl-CoA was added equimolar with flavin under anaerobic conditions, and the decrease of flavin absorbance was allowed to reach equilibrium (80 min) (Figure 10C). FcPF<sub>6</sub> was then added in a 10-fold molar excess over flavin. Approximately half of the initial flavin absorbance was immediately recovered, suggesting that only half of the absorbance decrease was due



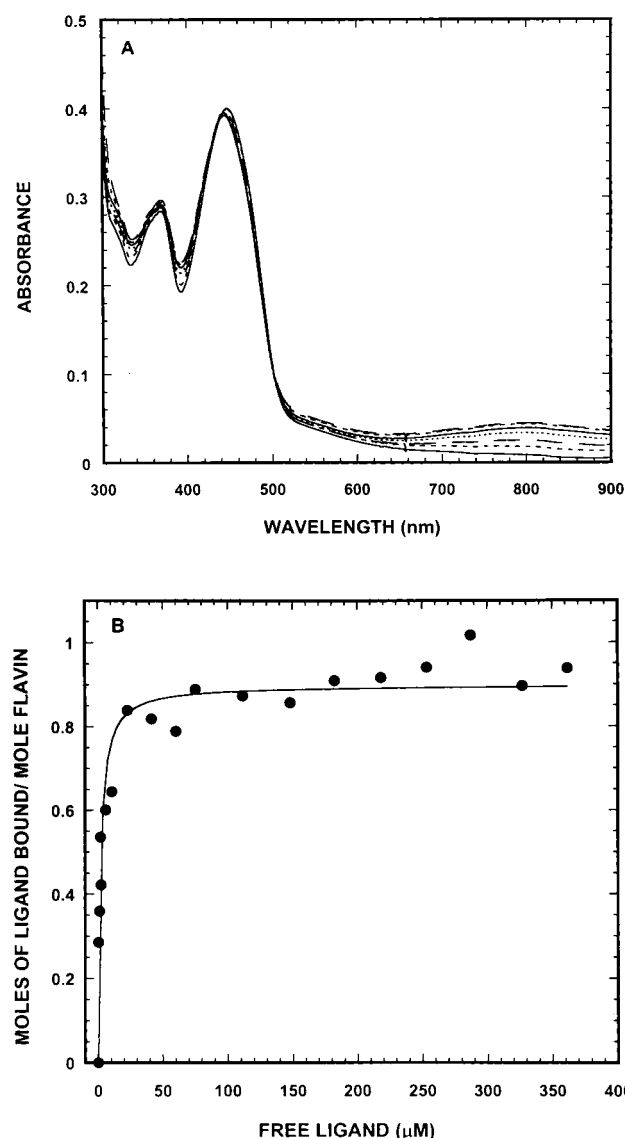


FIGURE 9: Spectrophotometric titration of Glu370Gln GCD with 3-thiaglutarlyl-CoA. (A) Absorption spectra of 30.3  $\mu$ M Glu370Gln GCD titrated with 3-thiaglutarlyl-CoA in 50 mM potassium phosphate, pH 7.0. (B) Data from panel A were plotted according to eq 1 in Experimental Procedures to determine the stoichiometry of binding (0.90) and the  $K_d$  (1.8  $\mu$ M).

to flavin reduction by substrate. On the basis of the crystal structure of GCD (9), the mechanism of deprotonation of 3-thiaglutarlyl-CoA and acetoacetyl-CoA by Glu370Gln GCD is not clear since there are no other potential base catalysts in the substrate binding site. The  $\alpha$ -proton of the analogue would be expected to be more acidic than the  $\alpha$ -proton of the substrate (38, 39). Although the equilibrium of the base-catalyzed removal of the  $\alpha$ -proton from the analogue by Glu370Gln GCD proceeds to a greater extent than that catalyzed by Glu370Asp GCD, the rate of proton abstraction is very slow with the Glu370Gln mutant, as judged by the data in Figure 10.

## DISCUSSION

The redox properties of human GCD are similar, but not identical, to other acyl-CoA dehydrogenases. The wild-type human GCD does not stabilize a neutral semiquinone when reduced photochemically or with sodium dithionite, unlike

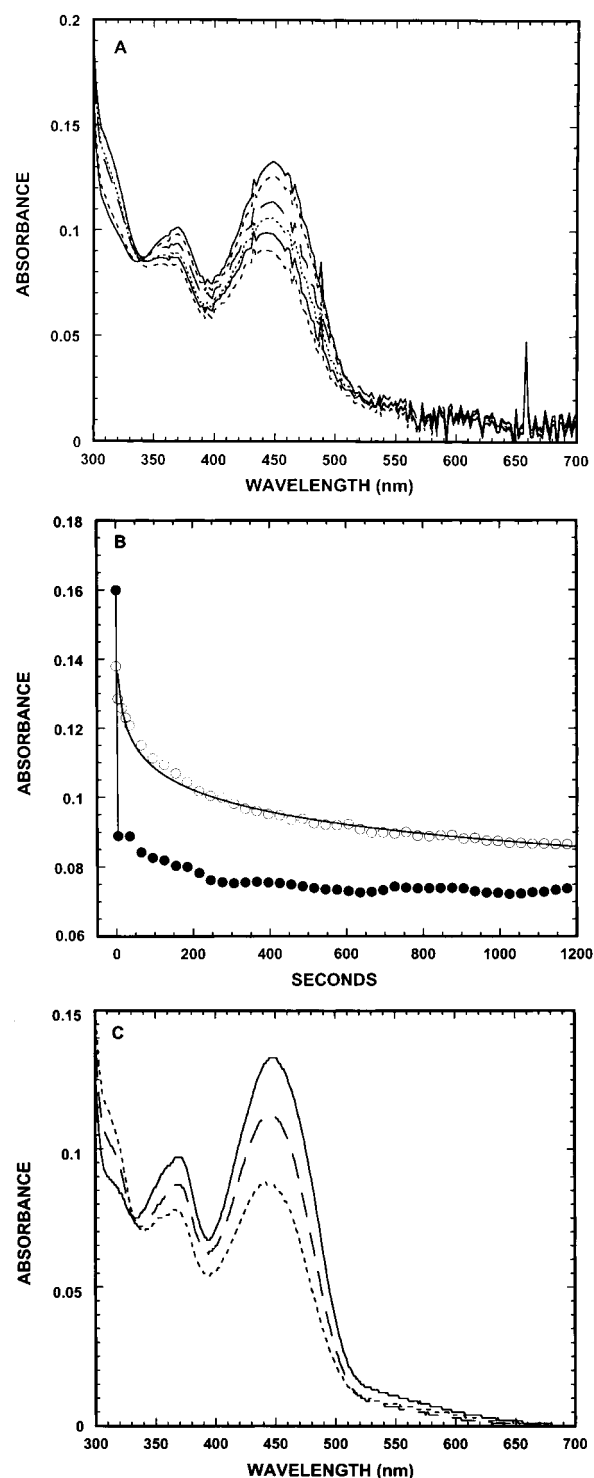


FIGURE 10: Reaction of glutaryl-CoA with wild-type and Glu370Gln GCD. (A) Absorption spectra of Glu370Gln GCD and (B) change in absorbance at 447 nm of 11  $\mu$ M wild-type (●) and 10.4  $\mu$ M Glu370Gln GCD (○). Some points are omitted for clarity. In the experiment shown in (A) and (B), the proteins were mixed with a 10-fold molar excess of glutaryl-CoA at 25 °C in 10 mM potassium phosphate, pH 7.6. The solid line in (B) indicates the fit of the data with Glu370Gln GCD to a single exponential. (C) Absorption spectrum of oxidized Glu370Gln GCD, 9.2  $\mu$ M, (—); spectrum of the mutant protein after addition of equimolar glutaryl-CoA recorded after 80 min (---); spectrum of the mutant protein reacted with 1 equiv of glutaryl-CoA for 80 min and after the addition of a 10-fold molar excess of FcPF<sub>6</sub> over dehydrogenase flavin (— · —). All reactions were conducted under anaerobic conditions, and anaerobic substrate and oxidant were added to the mutant enzyme as indicated.



medium-chain acyl-CoA dehydrogenase (17) and recombinant rat short-chain acyl-CoA dehydrogenase.<sup>2</sup> Like medium-chain acyl-CoA dehydrogenase (28), the enzyme stabilizes an anionic semiquinone in the presence of the enoyl-CoA product. Anaerobic reduction of the enzyme with glutaryl-CoA yields neither a neutral nor an anionic semiquinone. The extent of anaerobic reduction with substrate indicates an equilibrium between oxidized and reduced states of the flavin and acyl-CoA that is poised somewhat differently from most other acyl-CoA dehydrogenases. Addition of an equimolar concentration of glutaryl-CoA results in 23–26% reduction of the flavin; addition of a 10-fold excess of substrate reduced 63% of the flavin. In contrast, addition of equimolar substrates to *P. denitrificans* GCD, rat short-chain acyl-CoA dehydrogenase, pig kidney medium-chain acyl-CoA dehydrogenase, and human isovaleryl-CoA dehydrogenase reduced 59%, 61%, 53%, and 31% of the FAD prosthetic group, respectively (4, 11, 19, 13). In this respect, the redox equilibrium of human GCD appears similar to that of human isovaleryl-CoA dehydrogenase. The potential of free GCD is similar to, but slightly lower than, other dehydrogenases. Also, enoyl-CoA binding may not regulate the potential of the flavin in the human GCD to the same extent as other flavoprotein dehydrogenases (4, 22, 31). For example, enoyl-CoA product binding increases the potential of medium-chain acyl-CoA dehydrogenase and bacterial short-chain acyl-CoA dehydrogenase by 0.06 and 0.110 V, respectively (22, 31, 41). Byron et al. showed that the potential of *P. denitrificans* GCD increases 0.030 V in the presence of equimolar butyryl-CoA and crotonyl-CoA (4). However, the bacterial enzyme possesses significant enoyl-CoA hydratase activity, and there is significant hydration of crotonyl-CoA to 3-hydroxybutyryl-CoA. Therefore, although the substrate/product ratio can modulate the redox potential of the bacterial GCD flavin, the estimate of 0.03 V is considered qualitative (4).

Steady-state kinetic experiments with glutaryl-CoA, hexanoyl-CoA, and pentanoyl-CoA suggest that the  $\gamma$ -carboxylate of glutaryl-CoA contributes to the free energy of binding to the dehydrogenase. The degree of destabilization of the ES complex with hexanoyl-CoA or pentanoyl-CoA compared to glutaryl-CoA calculated from  $\Delta\Delta G = -RT \ln(K_m^{\text{glutaryl-CoA}}/K_m^{\text{acyl-CoA}})$  is 5.7 and 7.4 kJ/mol, respectively (42). The transition state for the overall oxidation of glutaryl-CoA is likely to differ from those of pentanoyl-CoA and hexanoyl-CoA because oxidation of glutaryl-CoA also involves tight binding of the glutaconyl-CoA intermediate, decarboxylation of glutaconyl-CoA, protonation of the  $\gamma$ -carbon, and dissociation of CO<sub>2</sub>. Therefore, it is not possible to compare the changes in Gibbs free energies directly from the steady-state constants. However, it is possible to calculate relative destabilization of the respective transition states, ES<sup>‡</sup>, in the overall oxidation of the acyl-CoA substrates. Destabilization of the transition state complexes with hexanoyl-CoA or pentanoyl-CoA is calculated from  $\Delta\Delta G^\ddagger_T = -RT \ln[(k_{\text{cat}}/K_m^{\text{acyl-CoA}})/(k_{\text{cat}}/K_m^{\text{glutaryl-CoA}})]$  (42). This approach yields a difference of 4.6 kJ/mol for the hexanoyl-CoA complex and a difference of 6.4 kJ/mol for the pentanoyl-CoA complex with respect to the transition state complex for glutaryl-CoA oxidation. Thus, GCD exemplifies an enzyme that uses the free energy of binding of the ES complex to increase the

second-order rate constant ( $k_{\text{cat}}/K_m$ ). The relative stabilization of the ES and ES<sup>‡</sup> complexes with glutaryl-CoA may result from interaction of the  $\gamma$ -carboxylate of both glutaryl-CoA and the presumed intermediate, glutaconyl-CoA, with Arg94 and, perhaps, Ser98, which lie at the “bottom” of the substrate binding site (9). Arg94 in glutaryl-CoA dehydrogenase is unique among the acyl-CoA dehydrogenases. The corresponding residues in human medium-chain acyl-CoA (43), rat short-chain acyl-CoA (11), and human isovaleryl-CoA dehydrogenases (44) are Gln95, Gly89, and Gly94, respectively. Arg94 may also stabilize the transient crotonyl-CoA anion, which must be protonated by the conjugate acid of Glu370 glutamate after decarboxylation (2). Mutation of Arg94 to glycine is pathogenic and causes glutaric acidemia type I (7). In contrast to the results with the alternate substrates, the Glu370Asp mutation does not affect substrate binding because the  $K_m$  for glutaryl-CoA is identical to that of wild-type GCD. Rather, the ~16-fold decrease of  $k_{\text{cat}}$  at pH 7, relative to the wild-type enzyme, indicates that the Glu370Asp mutation affects  $\Delta G^\ddagger$  (42).

The activity of wild-type GCD exhibits triphasic behavior within the pH range 6–9.5 in which the enzyme is stable during steady-state kinetic assays. This behavior is quite unlike the pH dependence of  $k_{\text{cat}}$  of human and porcine medium-chain acyl-CoA dehydrogenases and human long-chain acyl-CoA dehydrogenase reported by Kumar et al. and Ghisla et al. (45, 46). The  $k_{\text{cat}}$  of those dehydrogenases shows a single ionizable group ( $\text{p}K_a \approx 8.2$ ) over the pH range 6–10.5 with little change in  $K_m$  to at least pH 9.1 (45). This pH dependence does not reflect the rate of flavin reduction or oxidation in medium-chain acyl-CoA dehydrogenase. Rather, the off rate of the octenoyl-CoA product appears to limit  $k_{\text{cat}}$  (45). The steady-state turnover of GCD is more complex. In addition to the steps common to other acyl-CoA dehydrogenases, steady-state turnover of GCD also requires tight binding of the intermediate oxidized product, glutaconyl-CoA. The investigations of the pH dependence of GCD activity were conducted with 200  $\mu\text{M}$  glutaryl-CoA so that the measured activity probably reflects  $k_{\text{cat}}$  because the  $K_m$  for glutaryl-CoA does not increase significantly between pH 6 and pH 8, although the  $K_m$  increases to 35  $\mu\text{M}$  at pH 8.8. In the experiments reported here with human GCD, the first phase over the pH range 5.5–7.5 shows an ionizable group with  $\text{p}K_a = 6.3$ . The second phase, pH 7.5 to ~9.0, indicates an ionizable group with  $\text{p}K_a = 7.9$ , which is similar to the single  $\text{p}K_a$  observed with medium-chain and long-chain acyl-CoA dehydrogenases (46). The lower  $\text{p}K_a$ , at 6.3, may reflect protonic equilibria involved in the decarboxylation that requires proton transfer from Glu370 to the crotonyl-CoA anion (2) and is not observed with other dehydrogenases that catalyze only  $\alpha,\beta$  dehydrogenation.

In contrast to data with the wild-type dehydrogenase, a single ionizing group is observed over the same range (pH 5–8.2) for the Glu370Asp dehydrogenase with  $\text{p}K_a = 7.6$ . In preliminary experiments, we showed that crotonyl-CoA is also the product of the reaction catalyzed by Glu370Asp GCD.<sup>3</sup> No glutaconyl-CoA was detected, indicating that this enoyl-CoA intermediate is not released before decarboxylation occurs in the reaction catalyzed by Glu370Asp GCD. Thus, the overall steady-state pathway is apparently identical

<sup>2</sup> D. Zapfen and F. E. Frerman, unpublished data.

<sup>3</sup> F. E. Frerman, unpublished data.

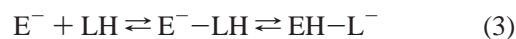
to the reaction catalyzed by wild-type GCD. The monophasic pH dependence of the Glu370Asp GCD between pH 5 and pH 8.2 may be due to differential effects of pH on the dehydrogenation reaction and decarboxylation reaction such that the effects of pH on turnover with the mutant cannot be distinguished. As pointed out above, the steady-state reactions of the two dehydrogenases are apparently identical. The failure to distinguish two  $pK_a$ s with Glu370Asp GCD could reflect one or more of the following differences between wild-type and Glu370Asp GCDs. The difference in distance between the carboxylate and the substrate in the two enzymes is on the order of  $\sim 1$  Å. Further, the orientation of the carboxylate of Asp370 with respect to the substrate  $\alpha$ -proton may be different from the orientation of the  $\gamma$ -carboxylate of Glu370 GCD and the proton (47), or there may be a small difference ( $\sim 0.5$  pH unit) between the  $pK_a$  of the  $\gamma$ -carboxyl of glutamate and the  $\beta$ -carboxylate of aspartate (48).

The ionizable group with a  $pK_a$  of  $\geq 9$  was not estimated because of the relative instability of the enzyme, substrate, and indicator dye in this pH range. The activities of both wild-type and Glu370Asp GCDs decrease above pH 8.5. This decrease is not observed in the steady state with medium-chain acyl-CoA dehydrogenases or long-chain acyl-CoA dehydrogenase (44, 45). However, rapid reaction experiments showed that the rate of deprotonation of (4-nitrophenyl)-acetyl-CoA by medium-chain acyl-CoA dehydrogenase decreases at higher pH ( $pK_a = 7.8$ ) (49). Also, the polarization of cinnamoyl-CoA due to ionization of Glu376 decreases at higher pH ( $pK_a = 8.5$ ) (50). In the case of GCD, polarization may be required not only to decrease the  $pK_a$  of the  $\alpha$ -proton of the substrate (41) but also to stabilize the intermediate crotonyl-CoA anion by delocalizing negative charge. It is also possible that Arg94 in human GCD may titrate with an abnormally low  $pK_a$  (i.e., in the range of pH 9) as observed in glyceraldehyde phosphate dehydrogenase and *Candida albicans* phosphomannose isomerase (51, 52).

In addition to a comparison of the steady-state kinetic properties of the mutant with the wild-type enzyme (see below), we investigated the binding and deprotonation of the substrate analogues, acetoacetyl-CoA and 3-thiaglutarlyl-CoA. These studies were undertaken because of the role of substrate deprotonation in the reductive half-reaction of the flavin and subsequent transfer of the proton to the  $\gamma$ -carbon of the crotonyl-CoA anion intermediate (2). The binding of acetoacetyl-CoA was investigated at pH 6.4, 3 pH units below the apparent  $pK_a$  for the enolization of 3-oxoacyl-CoA in solution (35). The apparent  $K_d$  of the binary complex is  $0.48 \mu\text{M}$ , calculated from changes in absorbance at 322 and 440 nm. The former absorbance is presumably due to enolate formation and the latter due to flavin perturbation by acyl-CoA binding. The free enolate absorbs in the region of 303 nm; however, the molar extinction of divalent metal chelates of the enolate in solution increases, and the maximum red shifts by at least 7 nm. The absorbance of the enolate at 322 nm indicates that the environment of the bound enolate is different from those environments of aqueous solution (35), the medium-chain acyl-CoA dehydrogenase binding site (53), and the Glu370Asp GCD mutant dehydrogenase.

The work of Tamaoki et al. (37) clearly shows that 3-thiooctanoyl-CoA binding and deprotonation by medium-chain acyl-CoA dehydrogenase occur according to the

equilibrium shown in eq 3. The charge-transfer band ( $\lambda_{\text{max}}$



$\approx 825$  nm) is due to the interaction of the analogue anion,  $\text{L}^-$ , with the oxidized flavin. The absorbance at 825 nm is, therefore, more properly a measure of deprotonation equilibrium. The  $pK_a$  of the corresponding enolate of 3-thiooctanoyl-CoA has been estimated at 5.2–5.7 when bound to medium-chain acyl-CoA dehydrogenase (37, 49). The pH dependence of  $\epsilon_{825\text{nm}}$  in the GCD–3-thiaglutarlyl-CoA complex indicates the participation of two ionizable groups with  $pK_a$ s = 7.0 and 8.2. The value of  $\epsilon_{825\text{nm}}$  reaches a maximum at pH  $\sim 8$  and then declines. These data suggest that the  $pK_a$  of the bound glutaryl-CoA analogue may be 1.5 pH units greater than the corresponding octanoyl-CoA analogue bound to medium-chain acyl-CoA dehydrogenase. Because the formation of the charge-transfer complex is exclusively due to proton abstraction at the  $\alpha$ -carbon, an elementary step in the reaction mechanism (54), the  $pK_a$ s, 7.0 and 8.2, can be ascribed to either (a) abstraction of the  $\alpha$ -proton of 3-thiaglutarlyl-CoA after binding to the active site of the enzyme or (b) protonation of the base catalyst, Glu370. However, it is not easy to unequivocally assign this  $pK_a$  to either of these processes. The  $\alpha$ -proton of acyl-CoAs is only weakly acidic in aqueous solution with an estimated  $pK_a$  of  $20 \pm 2$  (55–57). The 3-thia sulfur of 3-thiooctanoyl-CoA lowers the  $pK_a$  of the adjacent  $\alpha$ -proton by about 5 pH units compared to octanoyl-CoA (37, 58). Thus, a  $pK_a$  of 15–16 for the  $\alpha$ -proton of 3-thiaglutarlyl-CoA in solution is a reasonable estimate because it is unlikely that the  $\gamma$ -carboxylate significantly influences the ionization of the  $\alpha$ -proton. On the basis of molecular modeling of glutaryl-CoA into the crystal structure of wild-type GCD (9) and by analogy with the medium-chain acyl-CoA dehydrogenase–substrate complex, it is expected that the thioester carbonyl of glutaryl-CoA is hydrogen bonded to the 2'-hydroxyl of FAD and the backbone amide hydrogen of Glu370 and that the active site will be desolvated (43, 59). The resulting polarization of the thioester carbonyl would further activate the  $\alpha$ -proton for abstraction. The  $\gamma$ -carboxylate of free glutamate has a  $pK_a \approx 4.6$  (60). When buried in the protein, the  $\gamma$ -carboxyl of Glu370 in GCD would likely experience an increase in  $pK_a$  (48, 49, 58), especially if the active site is desolvated upon substrate binding (61, 62). At pH 8.0 the concentration of the charge-transfer-inducing anionic form of 3-thiaglutarlyl-CoA is significantly reduced (2.4%) when bound to Glu370Asp GCD. The primary cause of the decreased extent of charge-transfer complex formation is very likely the increased distance for proton transfer. However, the lower  $pK_a$  ( $\approx 0.5$  pH unit) of the aspartate  $\beta$ -carboxylate (48), relative to the  $\gamma$ -carboxylate of glutamate, may also be a factor. Proton abstraction at the  $\alpha$ -carbon appears highly concerted with hydride transfer to the flavin in medium-chain acyl-CoA dehydrogenase (2, 63). The decrease in turnover of the Glu370Asp GCD may be due, at least in part, to the unfavorable equilibrium for formation of the C- $\alpha$  anion.

The kinetic experiments reported here with the Glu370Asp and Glu370Gln GCDs strongly suggest that Glu370 is the catalytic base of human GCD. First, as pointed out by Kim et al. (9, 64), Glu370 is positioned identically with respect to substrate as the glutamate residues suggested to function

as catalytic bases in related acyl-CoA dehydrogenases. Second, the steady-state rates of the Glu370Gln and Glu370Asp GCD mutants are similar to those of the corresponding mutants in medium-chain acyl-CoA dehydrogenase (35) and long-chain acyl-CoA dehydrogenase (12). The Glu370Asp mutation apparently does not alter the catalytic mechanism,<sup>3</sup> and the  $K_m$  of Glu370Asp for glutaryl-CoA is the same as the wild-type value. Further, direct observation of the rate of flavin reduction by substrate of the Glu370Gln GCD shows that it is very slow, similar to that of the Glu376Gln mutant of medium-chain acyl-CoA dehydrogenase (34). Third, like *P. denitrificans* GCD (5), wild-type human GCD is very rapidly and irreversibly inhibited by the mechanism-based inhibitor, 2-pentynoyl-CoA,<sup>4</sup> suggesting that the catalytic base is positioned as described for medium-chain acyl-CoA dehydrogenase and not in the positions occupied by the catalytic glutamate residues in isovaleryl-CoA dehydrogenase [Glu254 (44)] and long-chain acyl-CoA dehydrogenase [Glu261 (12)]. Fourth, titration of the Glu370Gln mutant with substrate shows no development of a charge-transfer species ( $\lambda_{max} = 560$  nm), although a low level of reduction is observed since addition of FcPF<sub>6</sub> results in some increase in absorbance in the 448 nm region of the flavin absorption spectrum of Glu370Gln GCD. Some reduction of the flavin prosthetic group is expected in view of the residual activity of the protein. It is possible that other alterations within the active site could cause the decreased rate of catalysis by the two mutants. However, the fact that the flavin spectra are not significantly altered, the  $K_m$  of Glu370AspGCD for glutaryl-CoA is not altered, and the redox potential of the mutants is not significantly altered argues that the active sites of the two mutants are not significantly altered.

The spectral properties of the complexes of Glu370Gln GCD with acetoacetyl-CoA and 3-thiaglutaryl-CoA indicate that another pathway of deprotonation is available in this mutant protein. The maximum value of  $\epsilon_{825nm}$  at pH 7 suggests that the equilibrium for deprotonation of 3-thiaglutaryl-CoA by Glu370Gln GCD is not as favorable as with the wild-type enzyme. Substitution of Glu370 by glutamine would not be expected to decrease the polarization of substrate or 3-thiaglutaryl-CoA and the acidity of the  $\alpha$ -proton resulting from hydrogen bonding of the thioester oxygen to the 2'-hydroxyl of FAD (41, 50). Attempts to compare the difference between the intensities of charge-transfer complexes of Glu370Asp and Glu370Gln GCD's with steady-state rates of the two mutant enzymes may be misleading. The complexes with 3-thiaglutaryl-CoA were observed in equilibrium titrations, and we have not determined rate constants for deprotonation by the two mutant dehydrogenases. Despite the deprotonation of the two substrate analogues containing  $\alpha$ -protons with considerably lower  $pK_a$ s than glutaryl-CoA in solution and likely on the enzyme, the deprotonation of substrate by Glu370Gln GCD is not efficiently coupled with hydride transfer to the flavin. The similarity of the flavin spectrum of Glu370Gln GCD, its flavin redox potential, and its binding constants with acetoacetyl-CoA and 3-thiaglutaryl-CoA to the wild-type enzyme suggest that the active site of Glu370Gln GCD is probably not grossly altered and likely folded similarly to

wild-type GCD. Finally, the decrease in absorbance at 448 nm due to complex formation and some flavin reduction upon addition of substrate to the mutant enzyme is very slow, as previously demonstrated with the Glu376Gln mutant of medium-chain acyl-CoA dehydrogenase (34). It is not clear how deprotonation by the mutant protein occurs, although the Glu261Gln mutant of human long-chain acyl-CoA dehydrogenase behaves similarly in the deprotonation of acetoacetyl-CoA (12). The crystal structure does not indicate another catalytic base in the substrate binding site that could participate in this reaction (9). In addition to Arg94 and Ser98 at the bottom of the substrate binding site that may interact with the carboxylate of glutaryl-CoA and Glu370 that likely functions as the catalytic base, the active site is composed of side chains from Leu212, Val99, Leu103, Phe133, and Leu246 (9). It is possible that a water molecule may serve as an inefficient catalytic base in the turnover of Glu370Gln GCD.

Despite the high sequence homology (6) and similarity of three-dimensional structures (9, 64), the experiments reported here show clear differences between GCD and medium-chain acyl-CoA dehydrogenase, the best studied member in this family of flavoprotein dehydrogenases. They also suggest the role of the  $\gamma$ -carboxyl of glutaryl-CoA in substrate binding and its proposed interaction with Arg94 (9, 64). These studies serve to establish baseline properties of human GCD for ongoing investigations of the decarboxylation reaction catalyzed by the protein.

## ACKNOWLEDGMENT

We gratefully acknowledge the technical assistance of Ms. Loelle Poneleit and the assistance of Dr. Donald Zapien in the cyclic voltammetry experiments.

## REFERENCES

1. Lenich, A. C., and Goodman, S. I. (1986) *J. Biol. Chem.* 261, 4090–4096.
2. Gomes, B., Fendrich, G., and Abeles, R. H. (1981) *Biochemistry* 20, 1481–1490.
3. Husain, M., and Steenkamp, D. J. (1985) *J. Bacteriol.* 163, 709–715.
4. Byron, C. M., Stankovich, M. T., and Husain, M. (1990) *Biochemistry* 29, 3691–3700.
5. Schaller, R. A., Mohsen, A. A., Vockley, J., and Thorpe, C. (1997) *Biochemistry* 36, 7761–7768.
6. Goodman, S. I., Kratz, L. E., DiGiulio, Biery, B. J., Goodman, K. E., Isaya, G., and Frerman, F. E. (1995) *Hum. Mol. Genet.* 4, 1493–1498.
7. Goodman, S. I., Stein, D. E., Schlesinger, S., Christensen, E., Schwartz, M., Greenberg, C. R., and Elpeleg, O. N. (1998) *Hum. Mutat.* 12, 141–144.
8. Schwartz, M., Christensen, E., Superti-Furga, A., and Brandt, N. J. (1998) *Hum. Genet.* 102, 452–458.
9. Kim, J.-J. P., Wang, M., Paschke, R., Goodman, S. I., Biery, B. J., and Frerman, F. E. (1999) in *Flavins & Flavoproteins 1999* (Ghisla, S., Kroneck, P., Macheroux, P., and Sund, H., Eds.) pp 539–542, Rudolf Weber Agency for Scientific Publications, Berlin, Germany.
10. Lee, H. J., Wang, M., Paschke, R., Nandy, A., Ghisla, S., and Kim, J.-J. P. (1996) *Biochemistry* 35, 12412–12420.
11. Battaile, K. P., Mohsen, A. W., and Vockley, J. (1996) *Biochemistry* 35, 15356–15363.
12. Djordjevic, S., Dong, Y., Paschke, R., Frerman, F. E., Strauss, A. W., and Kim, J.-J. P. (1994) *Biochemistry* 33, 4258–4264.
13. Mohsen, A. W., and Vockley, J. (1995) *Biochemistry* 34, 10146–10152.

<sup>4</sup> T. M. Dwyer and F. E. Frerman, unpublished data.



14. Griffin, K. J., deGala, G. D., Eisenreich, W., Muller, F., Bacher, A., and Frerman, F. E. (1998) *Eur. J. Biochem.* 255, 125–132.
15. Simon, E. J., and Shemin, D. (1953) *J. Am. Chem. Soc.* 75, 2520.
16. Stadtman, E. R. (1957) *Methods Enzymol.* 3, 931–941.
17. Thorpe, C., Matthews, R. G., and Williams, C. H., Jr. (1979) *Biochemistry* 18, 331–337.
18. Beckmann, J. D., and Frerman, F. E. (1983) *J. Biol. Chem.* 258, 7563–7569.
19. Lehman, T. C., Hale, D. E., Bhala, A., and Thorpe, C. (1990) *Anal. Biochem.* 186, 280–284.
20. Watmough, N. J., Loehr, J. P., Drake, S. K., and Frerman, F. E. (1991) *Biochemistry* 30, 1317–1323.
21. Massey, V. (1991) in *Flavins and Flavoproteins 1990* (Curti, B., Ronchi, S., and Zanetti, G., Eds.) pp 59–66, Walter de Gruyter and Co., New York.
22. Lenn, N. D., Stankovich, M. T., and Liu, H. W. (1990) *Biochemistry* 29, 3709–3715.
23. Cantor, C. C., and Schimmel, P. R. (1980) *Biophysical Chemistry*, Part III, p 855, W. H. Freeman & Co., San Francisco, CA.
24. Fersht, A. (1999) *Structure and Mechanism in Protein Science*, pp 169–173, W. H. Freeman and Co., New York.
25. Sanger, F., Nicklen, S., and Coulson, A. R. (1977) *Proc. Natl. Acad. Sci. U.S.A.* 74, 5463–5467.
26. McKean, M. C., Beckmann, J. D., and Frerman, F. E. (1983) *J. Biol. Chem.* 258, 1866–1870.
27. Ghisla, S. (1980) *Methods Enzymol.* 66, 360–373.
28. Mizzer, J. P., and Thorpe, C. (1981) *Biochemistry* 20, 4965–4970.
29. Mancini-Samuelson, G. J., Kieweg, V., Sabaj, K. M., Ghisla, S., and Stankovich, M. T. (1998) *Biochemistry* 37, 14605–14612.
30. Clark, W. M. (1960) *Oxidation–Reduction Potentials of Organic Systems*, pp 184–203, Williams and Wilkins Co., Baltimore, MD.
31. Stankovich, M. T., and Soltysik, S. (1987) *Biochemistry* 26, 2627–2632.
32. Griffin, K. J. (1996) Ph.D. Dissertation, University of Colorado School of Medicine, Denver, CO.
33. Peterson, K. L., Galitz, D. S., and Srivastava, D. K. (1998) *Biochemistry* 37, 1697–1705.
34. Bross, P., Engst, S., Strauss, A. W., Kelly, D. P., Rasched, I., and Ghisla, S. (1990) *J. Biol. Chem.* 265, 7116–7119.
35. Stern, J. R. (1956) *J. Biol. Chem.* 221, 33–44.
36. Miura, R., Nishina, Y., Fujii, S., and Shiga, K. (1996) *J. Biochem. (Tokyo)* 119, 512–519.
37. Tamaoki, H., Nishina, Y., Shiga, K., and Miura, R. (1999) *J. Biochem. (Tokyo)* 125, 285–296.
38. Lau, S.-M., Brantley, R. K., and Thorpe, C. (1988) *Biochemistry* 27, 5089–5095.
39. Powell, P. J., and Thorpe, C. (1988) *Biochemistry* 27, 8022–8028.
40. Thorpe, C., and Kim, J.-J. P. (1995) *FASEB J.* 724, 718–725.
41. Stankovich, M. T., Sabaj, K. M., and Tonge, P. J. (1999) *Arch. Biochem. Biophys.* 370, 16–21.
42. Fersht, A. (1999) *Structure and Mechanism in Protein Science*, pp 349–376, W. H. Freeman and Co., New York.
43. Kim, J.-J. P., Wang, M., and Paschke, R. (1993) *Proc. Natl. Acad. Sci. U.S.A.* 90, 7523–7527.
44. Tiffany, K. A., Roberts, D. L., Wang, M., Paschke, R., Mohsen, A. W., Vockley, J., and Kim, J.-J. P. (1997) *Biochemistry* 36, 8455–8464.
45. Kumar, N. R., Peterson, K. L., and Srivastava, D. K. (1997) in *Flavins and Flavoproteins 1996* (Stevenson, K. J., Massey, V., and Williams, C. H., Jr., Eds.) pp 633–636, University of Calgary Press, Calgary, Canada.
46. Ghisla, S., Braunwarth, A., and Vock, P. (1997) in *Flavins and Flavoproteins 1996* (Stevenson, K. J., Massey, V., and Williams, C. H., Jr., Eds.) pp 629–632, University of Calgary Press, Calgary, Canada.
47. Nandy, A., Kieweg, V., Kräutle, F.-G., Vock, P., Küchler, B., Bross, P., Kim, J.-J. P., Rasched, I., and Ghisla, S. (1996) *Biochemistry* 35, 12402–12411.
48. Fersht, A. (1999) *Structure and Mechanism in Protein Science*, pp 188–189, W. H. Freeman and Co., New York.
49. Vock, P., Engst, S., Eder, M., and Ghisla, S. (1998) *Biochemistry* 37, 1848–1860.
50. Rudik, I., Ghisla, S., and Thorpe, C. (1998) *Biochemistry* 37, 8437–8445.
51. Kuzminskaya, E. V., Asryants, R. A., and Nagradova, N. K. (1991) *Biochim. Biophys. Acta* 1075, 123–130.
52. Wells, T. N. C., Scully, P., and Magnenat, E. (1994) *Biochemistry* 33, 5777–5782.
53. Auer, H. A., and Frerman, F. E. (1980) *J. Biol. Chem.* 255, 8157–8163.
54. Knowles, J. R. (1976) *Crit. Rev. Biochem.* 4, 165–173.
55. Trivel, R. C., Wang, R., Anderson, V. E., and Thorpe, C. (1995) *Biochemistry* 34, 8597–8605.
56. Amyes, T. L., and Richard, J. P. (1992) *J. Am. Chem. Soc.* 114, 10297–10302.
57. Fedor, L., and Gray, P. H. (1976) *J. Am. Chem. Soc.* 98, 783–787.
58. Bordwell, F. G., Van Der Puy, M., and Vanier, N. R. (1976) *J. Org. Chem.* 41, 1885–1886.
59. Engst, S., Vock, P., Wang, M., Kim, J.-J. P., and Ghisla, S. (1999) *Biochemistry* 38, 257–267.
60. Tanford, C. (1962) *Adv. Protein Chem.* 17, 69–165.
61. Gilbert, H. F. (1980) *J. Am. Chem. Soc.* 102, 7059–7065.
62. Gilbert, H. F. (1981) *Biochemistry* 20, 5643–5649.
63. Ghisla, S., Thorpe, C., and Massey, V. (1984) *Biochemistry* 23, 3154–3161.
64. Kim, J.-J. P., Wang, M., Paschke, R., and Roberts, D. (1999) in *Flavins and Flavoproteins 1999* (Ghisla, S., Kroneck, P., Macheroux, P., and Sund, H., Eds.) pp 491–498, Rudolf Weber Agency for Scientific Publications, Berlin, Germany.

BI000700G